Electronic Supplementary Material (ESI) for Journal of Materials Chemistry A.

Electronic Supplementary Information (ESI)

A flame-retardant wood-based composite with magnesium-aluminium layered double hydroxides for efficient daytime radiative cooling

Guowei Li, Jiawei Huang, Jian Zhou, Yucheng Zhang, Chuchu Zhang, Zhenggang Rao *, Linfeng Fei *

School of Physics and Materials Science, Jiangxi Engineering Laboratory for Advanced Functional Thin Films, and Jiangxi Key Laboratory for Two-Dimensional Materials, Nanchang University, Nanchang, Jiangxi 330031, China

** Corresponding authors.*

E-mail addresses: feilinfeng@gmail.com (L. Fei); raozhenggang@ncu.edu.cn (Z. Rao)

(a) (b)

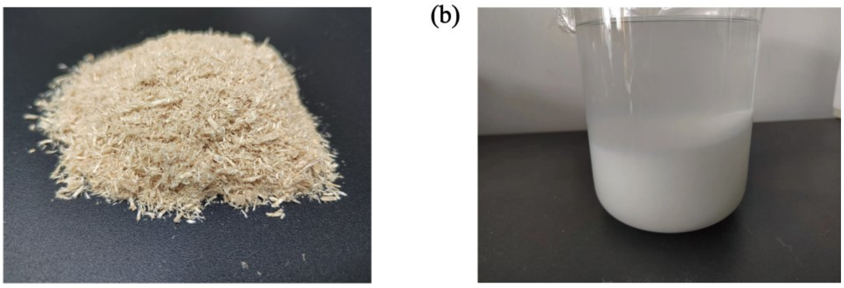

Figure S1. (a) Photograph for a pile of sawdust. (b) Photograph of lignocellulose dispersed in water.

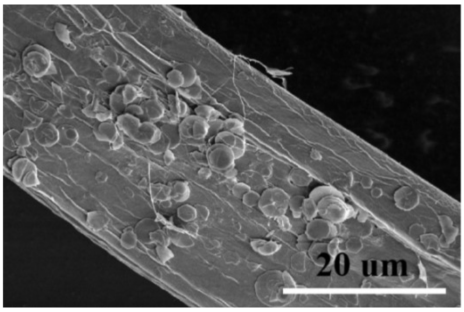

Figure S2. SEM image of MgAl-LDH nanoflakes loaded on a lignocellulose fiber.

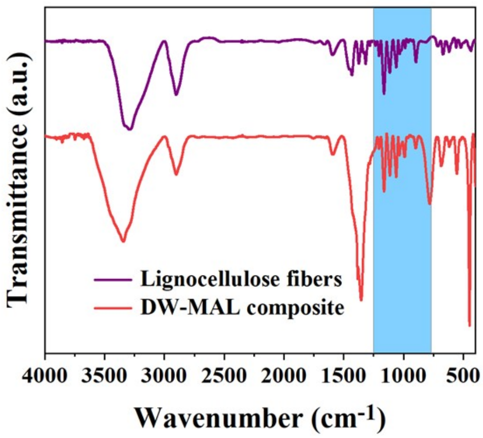

Figure S3. FTIR transmittance spectra of lignocellulose fibers and the DW-MAL composite. The absorption peaks observed at wavenumbers of 784 cm^{-1} (-OH) and 1063 cm^{-1} (CO_3^{2-}) are attributed to MgAl-LDH nanoflakes, while the peaks at 894 cm^{-1} (C-H), 992 cm^{-1} (C-O), 1110 cm^{-1} (C-H), and 1160 cm^{-1} (C-O-C) are associated with lignocellulose fibers.

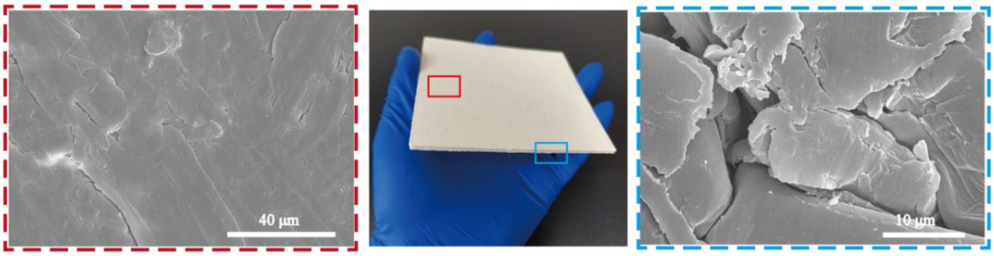

Figure S4. Frontview and sideview SEM images of a lignocellulose laminate.

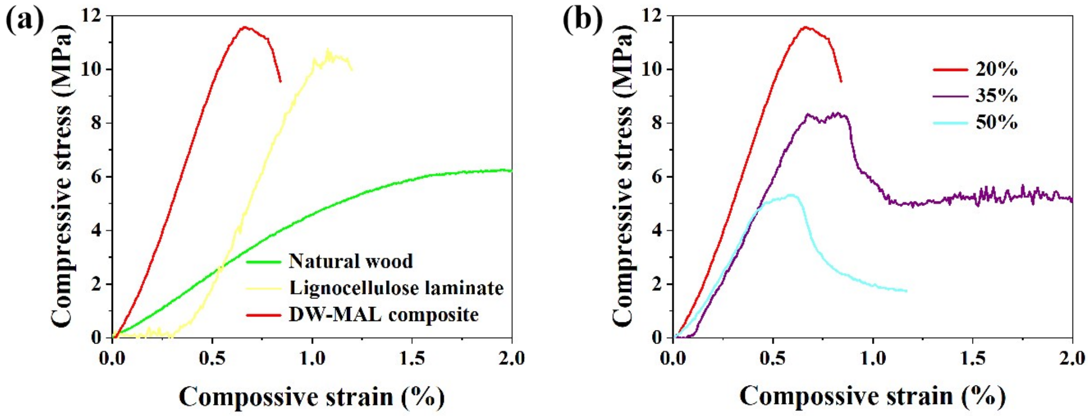

Figure S5. (a) Compressive stress-strain curves for natural wood, lignocellulose laminate and the DW-MAL composite. (b) Compressive stress-strain of the DW-MAL composite laminates with different MgAl-LDH contents.

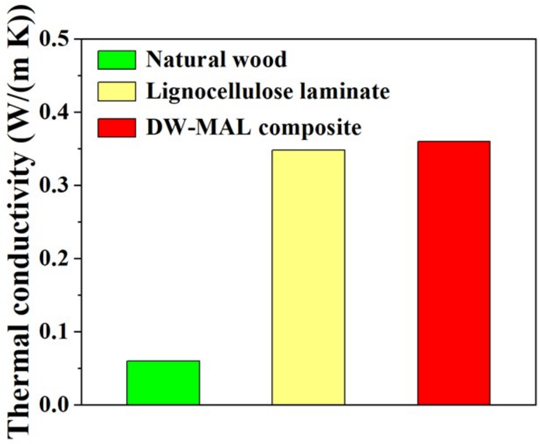

Figure S6. Comparison of thermal conductivities for natural wood laminate, lignocellulose laminate and the DW-MAL composite laminate.

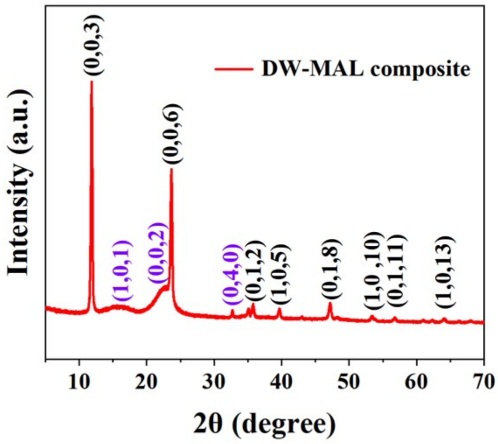

Figure S7. XRD pattern for the DW-MAL composite. The characteristic peaks marked in purple fonts belong to lignocellulose, while the peaks marked in black fonts belong to MgAl-LDHs.

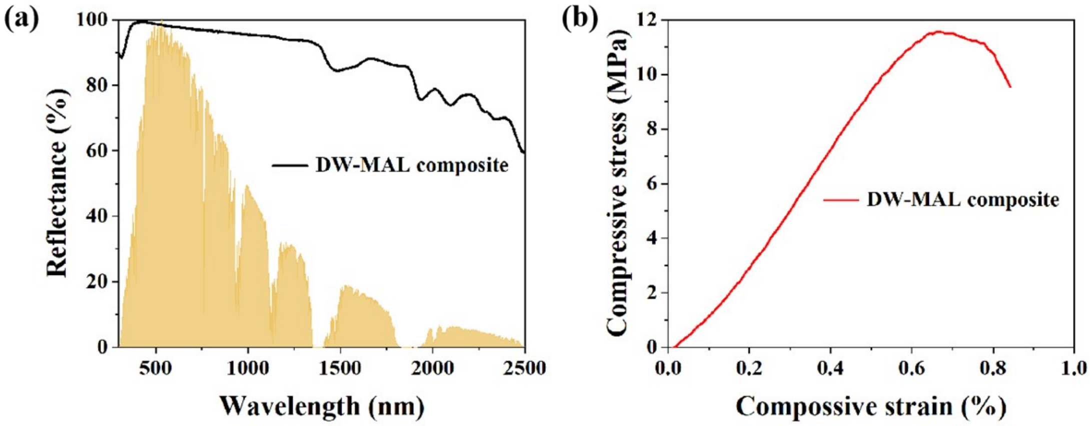

Figure S8. (a) Reflectance in solar spectrum for the DW-MAL composite after 6 months of storage. (b) Compressive stress-strain curve for the DW-MAL composite laminate after 6 months of storage.

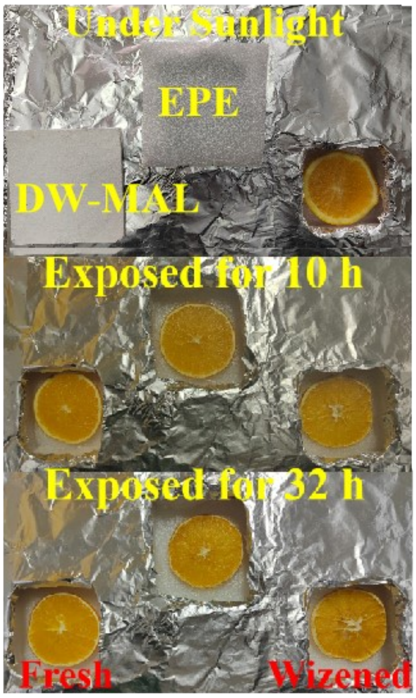

Figure S9. Orange preservations by the DW-MAL composite (the controlled groups were cover by a EPE foam or exposed to open air).

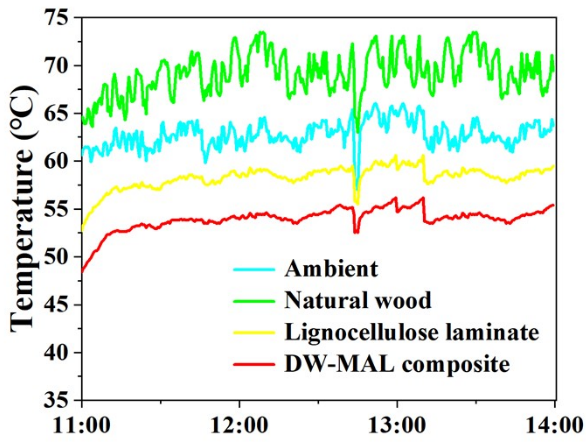

Figure S10. Comparative PDRC performance for natural wood, lignocellulose laminate, and the DW-MAL composite under sunlight. Be noted that this measurement was performed in another day as that of **Figure 3g**.

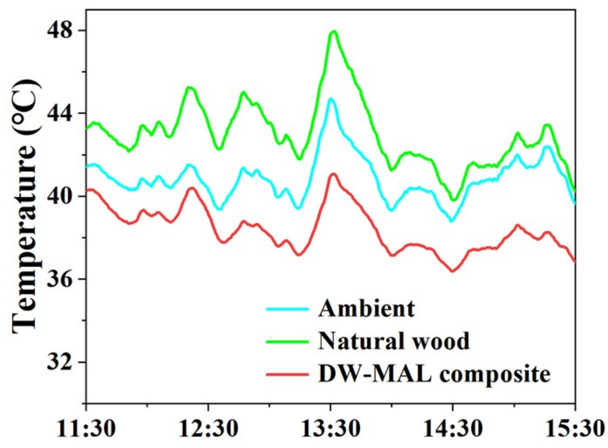

Figure S11. Comparative time-dependent surface temperature profiles for natural wood and the DW-MAL composite (tested after the removal of the topmost PE film as compared with **Figure 3g**).

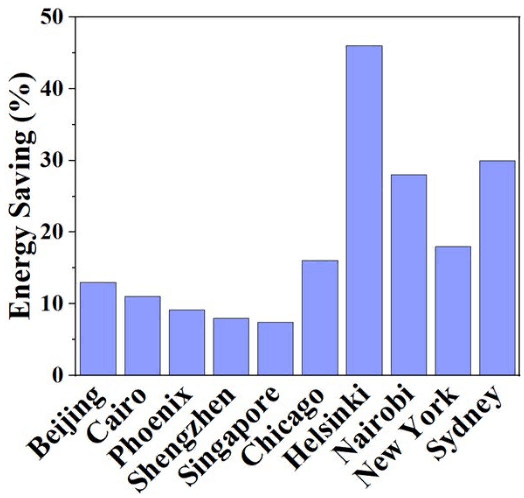

Figure S12. Building energy savings for ten representative cities around the world by using the DW-MAL composite.

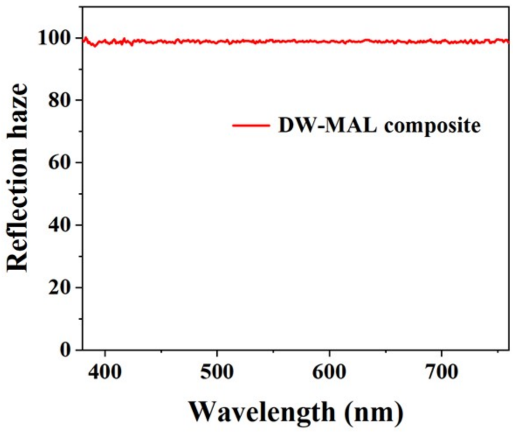

Figure S13. Reflection haze of the DW-MAL composite over visible wavelength.

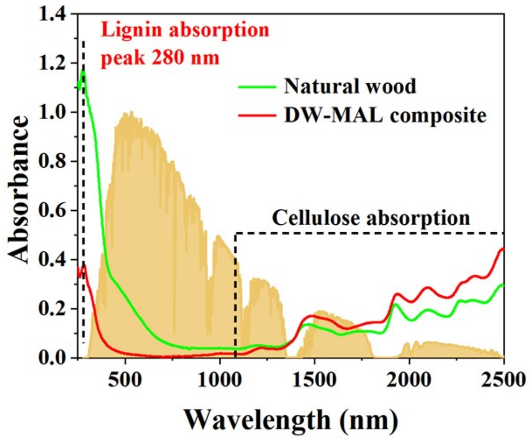

Figure S14. Absorbance v.s. wavelength profiles for the DW-MAL composite and natural wood.

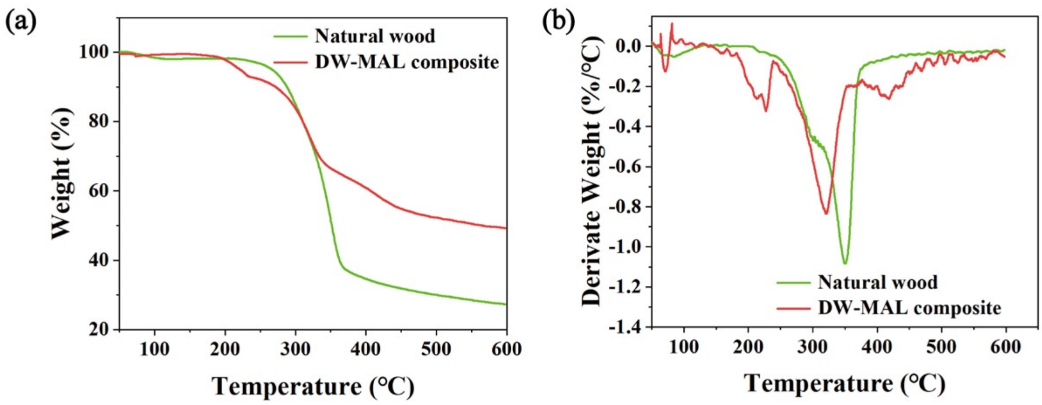

Figure S15. (a) TGA and (b) DTG profiles for natural wood and the DW-MAL composite. At the end of the thermal decomposition process, the DW-MAL composite retained a higher residual mass compared to natural wood.